DC MACHINES

Direct-current machines (dc machines) are used both as generators and motors. In the generator mode, mechanical input power at the rotating shaft is converted into electric output power at the electric terminals of the machine with an efficiency less than unity due to inevitable losses in the machine. Electrical output quantities are current and voltage. Both of them are dc values and may be used to feed electrical devices. In the motor mode, the energy flow is reversed: Electrical dc input power at the terminals is converted into mechanical output power at the rotating shaft, thus enabling the machine to drive a pump, an elevator, or a similar mechanical apparatus, again with an efficiency of less than unity.

BASIC DESCRIPTION OF DC MACHINES

These dc machines consist of a laminated iron core, fixed on a rotating shaft. An electrical armature winding is placed within slots along the circumference of the cylindrical rotor iron core near the surface; its coil ends are connected to the mechanical commutator, which consists of copper segments that are separated by electrically insulating thin mica sheets. The rotor, with its bearings mounted into bearing end shields, is rotating within the stator, which consists of several magnetic pole pairs (at least one pole pair is necessary). The stationary magnetic field of these poles in the airgap between stator and rotor induces an ac voltage (back emf) into the rotating armature winding according to Faraday's law (1,2). Carbon brushes, sliding on the commutator cylindrical surface, along with the commutator itself rectify the ac voltage, thus creating a dc voltage between two brushes of opposite electric potential. All positive brushes are connected to the positive terminal, and all negative brushes to the negative terminal likewise. If, for example, an ohmic resistor is connected to these terminals, a dc current will flow, and electric power will be dissipated as heat in the ohmic resistor. The machine is acting as a generator and needs mechanical input power to prolong the described power conversion. Inside the armature winding the current flow is—like the induced ac voltage—an ac current flow, which, along with the previously noted magnetic air-gap field, generates a constant braking torque according to Lorentz's law (1,2). Thus the mechanical input torque at the shaft, produced, for example, by a driving diesel engine, has to overcome the electromagnetic braking torque in order to generate energy flow from the diesel engine into the resistor.

By reversing the direction of power flow by reversing the direction of dc current flow outside the dc machine, one gets motor operation. For example, an external battery supply with a certain dc voltage sufficiently larger than the induced back emf to overcome the unavoidable voltage drop of internal end external electrical resistances will feed a dc current of opposite direction into the dc machine. The generated electromagnetic torque therefore also changes its direction and accelerates the rotor instead of the previously mentioned braking. Thus, the dc machine is able to drive other mechanically coupled machines such as pumps or elevators. So, both motor and generator operation are two modes of the same machine, depending on the direction of power flow.

The sliding brush–commutator mechanical contact (3) and the mechanically sensitive commutator itself put electrical and speed limitations to dc machines. Furthermore, brush wear under normal operation conditions, along with carbon dust production, requires maintenance such as changing the brushes that are too short and cleaning the machines to avoid electrical flashover within the windings due to the electrically conducting carbon dust layers. Therefore dc generators are currently replaced in many applications by ac synchronous generators with silicon rectifiers such as the electric generators in cars or rotating dc exciter units for large turbo generators in power plants (so-called "brushless" dc generators). As speed and torque of dc machines can be influenced separately by changing the applied voltage, thus changing the speed, or by changing the armature current, thus changing the torque, these machines are preferred as variable-speed drives. The control methods are simple, the produced torque is smooth, and dynamical response is very quick, as the electromagnetic time constant of the armature circuit is low. For many years these machines have been used as variable-speed drives in

numerous industrial applications such as steel mills, paper production, centrifugal drives, elevator drives, cranes, traction motors for electric railways, and motor–generator sets in submarines. These machines are both used in motor and generator mode, feeding back electric power to the grid during regenerative braking. Variable armature and field voltage is supplied by silicon-controlled rectifiers (thyristor bridges), thus enabling the machines to be operated also with weakened magnetic field to extend the speed range when the armature voltage limit is already reached. These power converter units are simple and therefore cheap, resulting in rather low acquisition costs for the combined machine–converter–control unit in spite of the fact that the machine itself is rather expensive due to the mechanically complicated rotor structure. Nevertheless, the decrease of costs for ac inverters, their improved switching performance due to improved power electronic devices such as insulated gate bipolar transistors (IGBT), and the advent of improved motor control for ac induction machines (so-called vector control) due to improved microcomputer technology led to a change from ac to dc drives. The induction motor is more robust, having only a squirrel cage in the rotor instead of the mechanical commutator and the wound armature winding, thus aiming for higher speed limits and resulting in higher dynamic performance due to the lower moment of inertia, at reduced maintenance costs (1). In the high-power region above 1 MW inverter-fed synchronous machines are also replacing large dc machines, as they allow a more compact build due to the lacking commutator. Larger ratios output power versus motor volume are achieved and higher mechanical speed is reached. For big dc drives, for example, two coupled machines (tandem motors) are necessary, whereas with ac synchronous drives there is only one machine needed. Still there is ample application of dc drives now, mainly in the power range of 100 kW up to 1000 kW due to the previously noted benefits. Their technical performance has steadily improved with benefits such as extended brush life, improved winding insulation, optimized cooling for a more compact build, and the use of on-line machine diagnostics to reduce maintenance (4,5).

BASIC EQUATIONS OF DC MACHINES

In Fig. 1(a) a simplified cross section of a two-pole dc machine is depicted (number of pole pairs $p = 1$). This simple machine has only one armature coil lying in two opposite slots at diameter d, with its ends connected to a simplified commutator with two copper segments. The machine—with its rotor turning with rotational speed n—acts as a dc generator at no-load condition, as there is no current flow in the armature, as no load is connected to the terminals. The north and the south pole air-gap magnetic field with peak flux density B induces an ac voltage (emf) u_i into the armature coil due to the movement of the coil sides with air-gap velocity v (length l of each coil side corresponding to the iron stack length and number of turns per coil N_c) [Fig. 1(b)]:

$$v = d\pi n \tag{1}$$

The rectified ac voltage u_i yields a dc voltage U_i, which for the

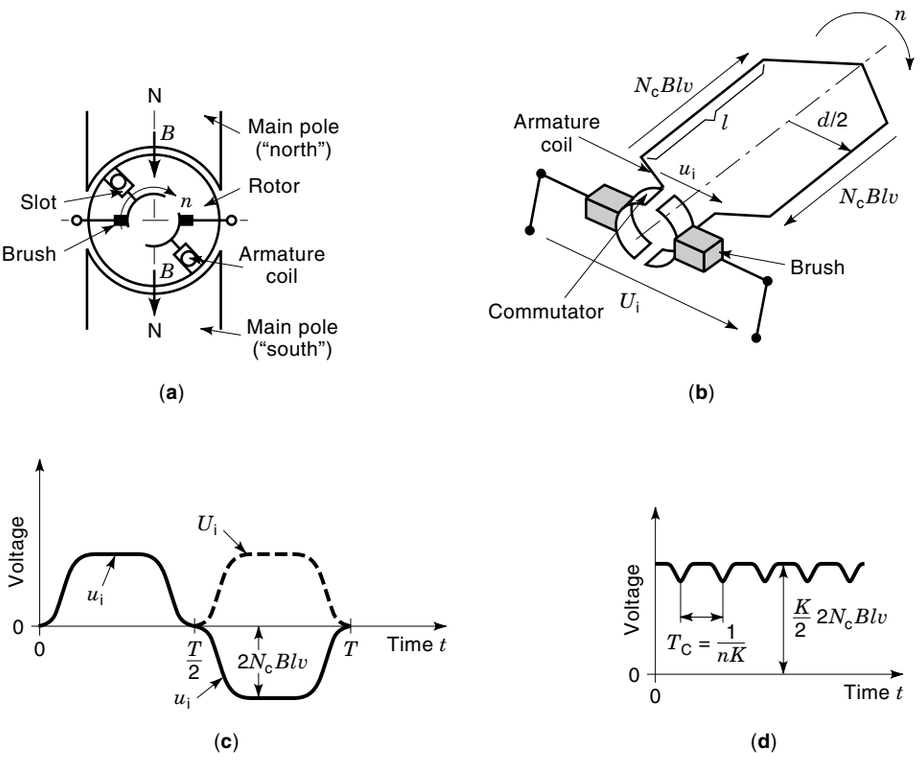

Figure 1. Simplified dc generator under no-load conditions with one pole pair, one armature coil, two commutator segments, and two brushes. (a) Cross section and air-gap field B. (b) Induced ac voltage u_i and rectification by the commutator U_i. (c) The nonuniform air-gap flux distribution causes a dc terminal voltage U_i with considerable ripple. (d) The voltage ripple gets smaller if more than one armature coil is connected in series ($K/2 > 1$).

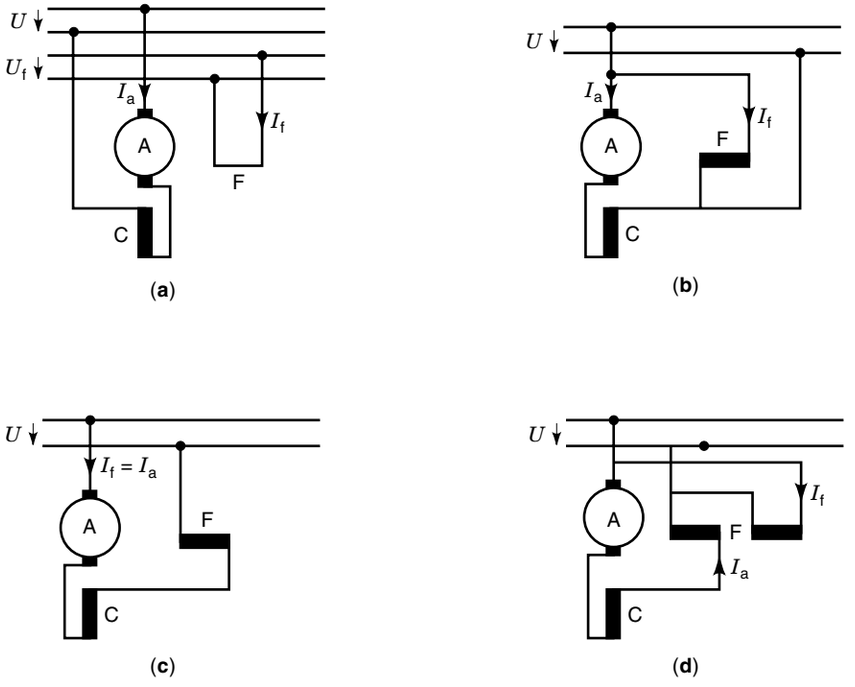

Figure 2. Different possibilities of connecting armature (A), compole (C), and field winding (F) to the dc grid. (a) Separate excitation. (b) Shunt excitation. (c) Series excitation. (d) Compound excitation.

"one-coil machine" shows a considerable ripple with armature frequency f_a [Fig. 2(c)]:

$$U_i = 2N_c Blv \tag{2}$$

$$f_a = np = \frac{1}{T} \tag{3}$$

In order to get a smooth dc voltage, usually many series connected coils are used instead of only one. These K coils—being placed in Q slots as a two-layer winding, resulting in $u = K/Q$ coils per slot and layer—are connected with both ends to K commutator segments, resulting in two parallel paths of $K/2$ series connected coils between the plus and minus brush, when a two-pole machine is considered. The induced ac voltages of adjacent armature coils are phase-shifted according to the displacement of one commutator pitch, yielding a superimposed ac ripple on the rectified voltage with commutator frequency f_C [Fig. 1(d)]. This ripple of typically 1% to 2% is lower the higher the ratio $K/(2p)$ is chosen (typically 30 to 40), yielding a nearly ideal dc voltage

$$f_C = Kn = \frac{1}{T_C} \tag{4}$$

Usually dc machines are manufactured with two or more pole pairs; thus the number of parallel paths $2a$ increases likewise when lap windings are chosen, Eq. (28). So one derives for the induced dc voltage equation (5), which depends on rotary speed n and the magnetic flux per pole Φ,

$$U_i = 2KN_c \frac{p}{a} n\Phi = kn\Phi \tag{5}$$

The equivalent pole arc ratio α_e (typically 0.7) considers the decrease of the air-gap field in the neutral zone,

$$\Phi = \alpha_e \frac{d\pi}{2p} lB \tag{6}$$

In the same way the expression for the electromagnetic torque M is derived when a current I_a (dc value outside the machine current) flows in the armature:

$$M = \frac{k}{2\pi} I_a \Phi \tag{7}$$

The terminal voltage U has to balance the emf and the voltage drop due to the armature resistance R_a and the brush voltage drop U_b, which typically is about 2 V for plus and minus brush, nearly independent of load current. Depending on machine operation mode (motor or generator) and thus polarity of armature current (positive or negative) one gets two expressions for the voltage equation (6,7).

Motor operation:

$$U = U_i + I_a R_a + U_b \tag{8}$$

Generator operation:

$$U = U_i - I_a R_a - U_b \tag{9}$$

MOTOR–GENERATOR SETS

Different possibilities of connecting the armature winding (A) and the stator field winding (F), which is exciting the electromagnetic poles via the field current I_f, to the dc grid are possi-

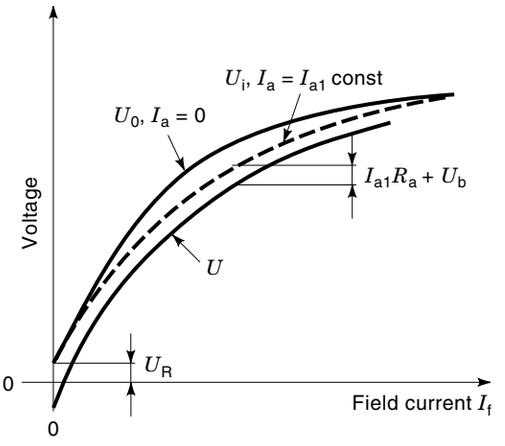

Figure 3. No-load characteristic of a dc generator for fixed rotational speed n: no-load voltage U_0, residual voltage U_R, induced voltage U_i under load with influence of an armature reaction, and terminal voltage U for variable field current I_f and fixed armature current I_a.

ble and in practical use (Fig. 2). Auxiliary windings (C) such as compole and compensating windings (see the section entitled "Armature Coils") are always connected in series to the armature winding. For clarification, in Fig. 2 no field rheostats or field shunts in the electric field circuit or starting resistors in the armature circuit are depicted. The field resistors are necessary to change the field current under fixed voltage-supply conditions, whereas the starting resistors are necessary to limit the armature current at motor standstill and during motor starting.

One distinguishes four different main-pole excitation methods both in motor and generator operation:

1. Separate excitation [Fig. 2(a)]
2. Shunt excitation [Fig. 2(b)]
3. Series excitation [Fig. 2(c)]
4. Compound excitation [Fig. 2(d)], which is a combination of methods 2 and 3

Equations (4) and (5) yield the corresponding external voltage–current characteristics of the generator mode and the speed–torque characteristics of the motor mode for the four different excitation modes. As a basic understanding of all these characteristics one has to consider first the open-circuit curve ($I_a = 0$), which gives the no-load voltage U_0 of a separately excited generator for fixed rotational speed n (Fig. 3). With increasing field current I_f the main flux per pole Φ and thus the emf U_i increases, too, but due to saturation of the iron parts (mainly the rotor teeth) beyond an air-gap flux density of about 1 T (corresponding to a tooth induction of about 1.8 T to 2 T) the curve bends, limiting the magnetic air-gap field. A certain iron hysteresis effect, resulting in two slightly different branches for increasing and decreasing field current, usually can be neglected. Only the effect of the stator iron remanent flux density has to be considered, yielding a small residual armature voltage U_R even at the open-circuited excitation circuit. With load ($I_a \neq 0$) an additional air-gap flux is excited by the loaded armature winding. At the main-pole tips the main flux density is either strengthened or weakened by this so-called armature reaction field. If there is no iron saturation, the average main-pole flux would remain unchanged. With a nonlinear iron characteristic there is additional load-dependent flux saturation in the teeth beneath the pole tips, where main flux and armature reaction flux are added with the same polarity. Therefore under load the resulting flux per pole is lower at high armature current values, yielding a lower induced voltage at load U_i than at no-load U_0 (Fig. 3). This armature reaction effect can be eliminated by using a compensating winding, placed in slots in the main-pole shoes opposite the armature rotor slots (Fig. 12).

Generator Characteristics

An external torque (generated by a turbine, a diesel engine, an electric motor, etc.) is driving the dc generator with fixed rotational speed n.

The load characteristic of the separately excited generator [Fig. 4(a)] is given for fixed field current, yielding a no-load voltage U_0, Eq. (5). According to Eq. (9) the terminal voltage U drops with rising load current I_a slightly due to the previously mentioned ohmic voltage drop. If the armature reaction is not compensated, an additional voltage drop occurs at high load values due to load-dependent iron saturation.

The decline of the load characteristic of the shunt generator [Fig. 4(b)] is larger than that of the separately excited generator, as the decreasing terminal voltage U is at the same time also the decreasing voltage at the field windings terminals, which leads to decreasing field current with increasing load. Below a certain value of field excitation the iron parts are unsaturated, giving two terminal voltage values for one certain armature current value. Thus a maximum current output exists.

From Fig. 3 one easily derives the load characteristic of the series generator [Fig. 4(c)], as armature and field current are identical. As the armature current is usually much larger than the field current of the separately excited generator, the series-connected field winding consists of few turns N_s, whereas with separate excitation this number N_f is large in order to reach the same magnetomotive force (mmf) $I_a N_s = I_f N_f$ with a low field current. Practical use of this type of generator is only under regenerative braking conditions of series motors, typically in electric vehicles and railway dc locomotives.

By combining both series and shunt excitation an almost load-independent output voltage between no-load and rated load can be achieved. Therefore this type of generator—along with the separately excited generator—are in practical use. Note that with the shunt generator it is possible to convert mechanical into electrical energy without any external electric source. The remanence induction, due to the rotation of the armature in this air-gap field, induces already at the no-load condition a certain residual voltage U_R (Fig. 3), which drives a small initial field current through the circuit resistance. Thus an electrically excited magnetic flux density buildup starts, amplifying the armature voltage, which again increases the field current up to a certain value at which the

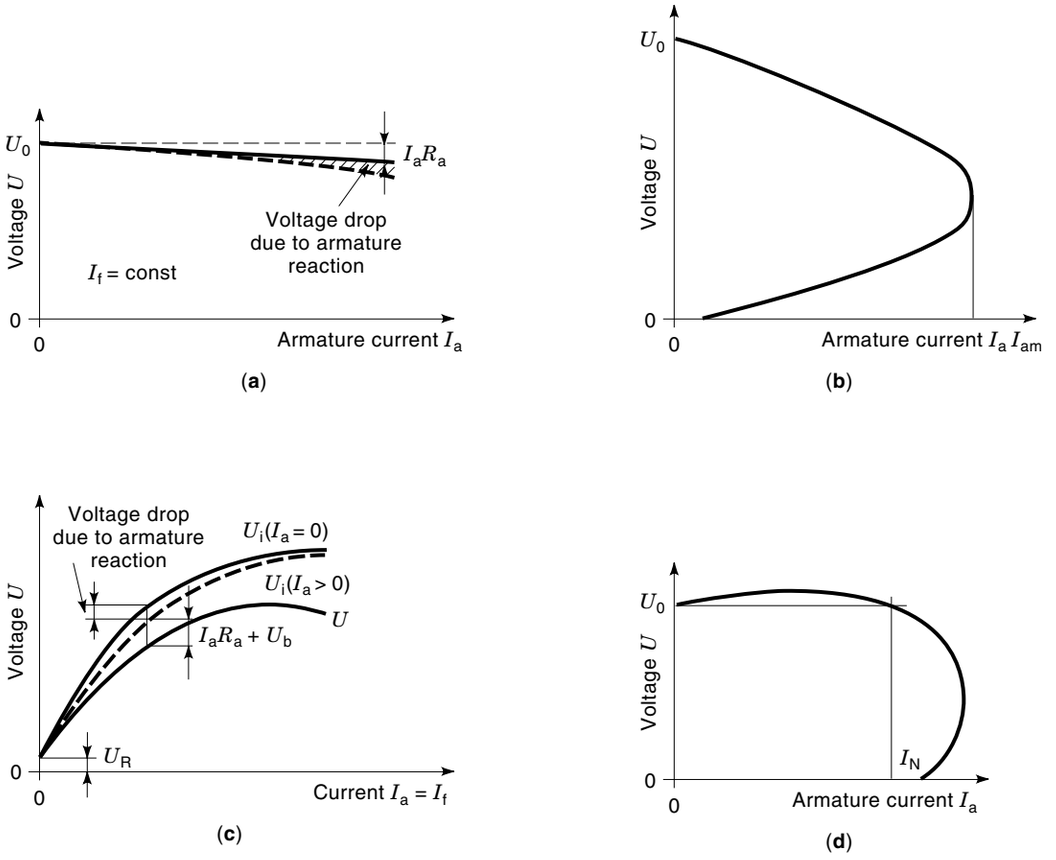

Figure 4. External characteristics of dc generators for fixed rotational speed n. (a) Separate excitation. (b) Shunt excitation. (c) Series excitation. (d) Compound excitation.

voltage drop along the circuit resistance and emf are equal. The discovery of this so-called self-excitation (*dynamoelectric principle*) by Werner von Siemens in 1866 was a revolution to electric power generation and was one of the main reasons for the breakthrough of electricity in industrial application. The same effect is now used for self-excitation of large synchronous power generators during startup after blackout, and also for self-excitation of synchronous and induction stand-alone generators, for example, in wind turbine application or emergency generating sets.

Motor Characteristics

In the following the motor terminal dc voltage U is assumed to be constant as well as the dc supply voltage U_f for the field circuit. Therefore, there is no basic difference between the separately excited motor and shunt motor. By combining Eqs. (5), (7), and (8), one derives the speed–torque characteristic of both types of motors (brush drop U_b for simplification neglected):

$$n = n_0 - \frac{2\pi R_a}{(k\Phi)^2} M \tag{10}$$

For simplification, the electromagnetic torque M is assumed to be the same as the shaft torque. Losses in the active rotor iron, eddy current losses in the rotor conductors due to the coil ac current, and inevitable friction losses cause a slightly smaller shaft torque (typically 1% to 2%). The decrease of speed with increasing torque is rather small [Fig. 5(a)], yielding a nearly constant speed with an upper value n_0 at the no-load condition:

$$n_0 = \frac{U}{k\Phi} \tag{11}$$

Flux drop at high torque (or at high armature current), caused by uncompensated armature reaction, will increase speed with increasing load, which might cause unstable motor operation for certain external load characteristics such as loads with speed-independent torque (for example, elevators and cranes). In these cases either a compensating winding or a motor-speed control is necessary.

Considering $I_a = I_f$ and thus $\Phi \propto I_a$ (constant saturation assumed), one gets from Eqs. (5), (7), and (8) the following steady-state characteristic for the series motor [Fig. 5(b)] with a strongly load-dependent speed decrease and a considerably large starting torque:

$$n \propto \frac{U}{\sqrt{M}} - \text{const} \tag{12}$$

Thus series motors are recommended drives for traction, either in battery-supplied electric vehicles and dc railway locomotives or in ac railway locomotives as single-phase commu-

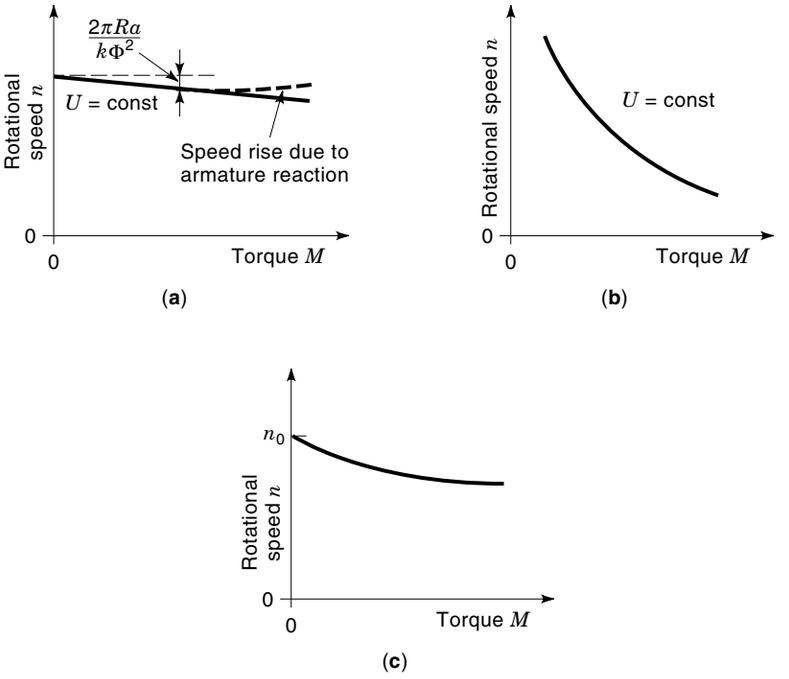

Figure 5. Speed–torque characteristics of dc motors for fixed armature voltage U. (a) Separate and shunt excitation, fixed field current I_f. (b) Series excitation. (c) Compound excitation.

tator motors, usually with series compensation winding. The reduction of field current has to be limited to prevent overspeeding with low loads. Series motors are well suited for being operated in parallel, supplied by one common electric source. For example, each of the four wheel sets in a four-axis locomotive is driven by a separate motor. Slight speed differences at the different wheel sets due to slip on wet rails results in only a slight difference in armature current consumption of the different motors due to the strongly load-dependent characteristic, Fig. 5(b). Separately excited motors would show large differences in armature current consumption due to the nearly load-independent characteristic, Fig. 5(a), leading to quick overheating of the motors with large current input. Therefore this type of motor is used in railway traction only with speed and current control.

Combining series and shunt excitation again yields a rather strongly load-dependent speed characteristic [Fig. 5(c)], but with the advantage of avoiding overspeeding with low loads. The shunt excitation ensures that speed cannot surpass the no-load speed n_0.

SOLID-STATE DRIVES

Usually there is no dc grid available to operate dc machines, as the power supply of today is performed by a three-phase ac line sinusoidal voltage u_L (amplitude $\sqrt{2}U_L$) with frequency f (50 Hz or 60 Hz). Before the advent of power electronics the necessary variable dc voltage was generated by a separately excited dc generator with variable excitation, driven by an induction motor, which was supplied by the ac line (so-called Ward–Leonard system) (1). Nowadays, silicon-controlled rectifiers (usually six-pulse thyristor power converters) are used (8,9). The ac line voltage is rectified by six-pulse silicon rectifiers [Fig. 6(a)] to generate a dc terminal voltage U. According to Eqs. (5) and (8) this voltage should be variable to get variable speed drives. Depending on the firing angle α (7) one gets a dc voltage U of variable amplitude with a superimposed ac voltage ripple [Fig. 6(b)]. As a result, the dc armature current also shows a considerable ripple with the frequency $6f$ (300 Hz or 360 Hz), which can be reduced by an additional series armature choke. Further improvements are possible by using 12-pulse converters (6). The power-converter arrangement of Fig. 6(a) allows only one direction of current flow, as the thyristors are blocking the reverse direction, but both positive and negative polarity of voltage U:

$$U = U_0 \cos(\alpha) \tag{13}$$

$$U_0 = \frac{3}{\pi}\sqrt{2}U_L \tag{14}$$

Rectifying the line voltage without any delay angle ($\alpha = 0$) yields the maximum voltage U_0. Usually the range for the thyristor delay angle is limited:

$$30^\circ \le \alpha \le 150^\circ \tag{15}$$

The upper limit 150° is given by the inverter stability limit. At 180° the inverter would shoot through (9). By defining a minimum angle of 30°, a voltage reserve between 87% and 100% of U_0, corresponding to angle values between 0° and 30°, remains for the speed controller. Thus the rated motor voltage is $U_N = 0.87U_0$. For motor operation in a clockwise rotation direction the delay angle is smaller than 90°, yielding a positive motor terminal voltage. With positive armature current flow direction, positive dc input power P_i

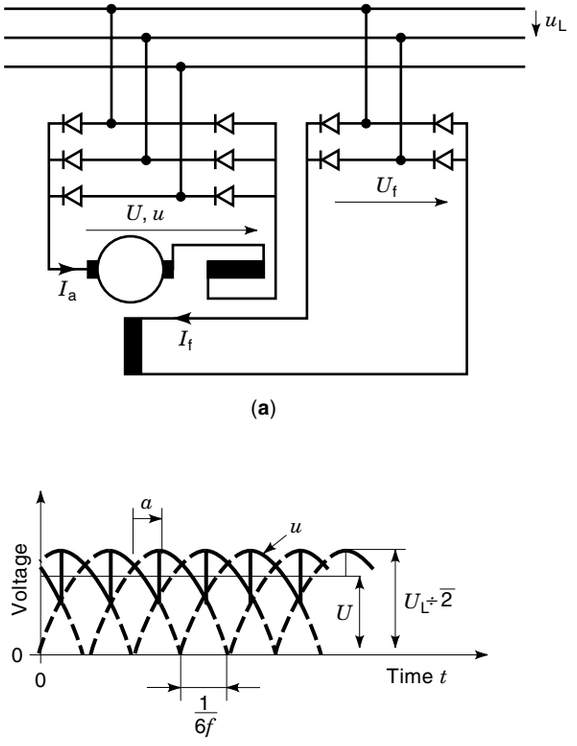

Figure 6. Converter-fed, separately excited dc machine. (a) Six-pulse converter for the armature circuit and two-pulse converter for the field circuit (first-quadrant operation). (b) Average voltage U is decreased by increasing the delay angle α.

$$P_i = UI_a \tag{16}$$

is transferred from the grid to the motor and converted into mechanical output power P_o:

$$P_o = 2\pi nM \tag{17}$$

With a firing angle α larger than 90° the voltage U becomes negative and the direction of speed will reverse from clockwise (cw) to counterclockwise (ccw) direction. As current and torque are still positive, the dc power becomes negative, too, thus becoming a power flow from the dc machine back to the grid. The dc machine acts as a regenerative brake. Motor operation with both cw and ccw speed is only possible if a second antiparallel controlled rectifier is added in Fig. 6(a). In that case the following values of speed, torque, voltage, and current are possible, while the main flux Φ is kept constant.

First quadrant—motor operation, converter 1 active:

$$n > 0, \qquad M > 0, \qquad U > 0, \qquad I_a > 0, \qquad \alpha_1 < 90^\circ$$

Second quadrant—generator operation, converter 2 active:

$$n > 0, \qquad M < 0, \qquad U > 0, \qquad I_a < 0, \qquad \alpha_2 > 90^\circ$$

Third quadrant—motor operation, converter 2 active:

$$n < 0, \qquad M < 0, \qquad U < 0, \qquad I_a < 0, \qquad \alpha_2 < 90^\circ$$

Fourth quadrant—motor operation, converter 1 active:

$$n < 0, \qquad M > 0, \qquad U < 0, \qquad I_a > 0, \qquad \alpha_1 > 90^\circ$$

By changing the delay angle α, the armature voltage U can be varied continuously, thus making it possible to run the drive with any selected pair (n,M) under steady-state conditions within the limits of rated torque M_N and maximum speed n_m. Rated torque is defined by the rated current I_N, which is a thermal limit to the armature, and the rated field current I_{fN}, which is both a thermal limit to the field coils and a saturation limit of the iron core. At rated speed n_N the maximum armature voltage, called the rated voltage U_N, is reached. Beyond this speed a further increase in speed is only possible, if—according to Eq. (5)—the main flux Φ is reduced by decreasing the field current I_f (field-weakening operation, Fig. 7). The armature current is kept constant, but the torque decreases with $1/n$, Eq. (7). The slope of speed decrease with increasing load is larger with weakened flux than with rated flux, Eq. (10).

Two different operation modes are possible and in use for antiparallel converter supply.

1. Both converters are active and produce the same average output voltage U, but only one of them provides the

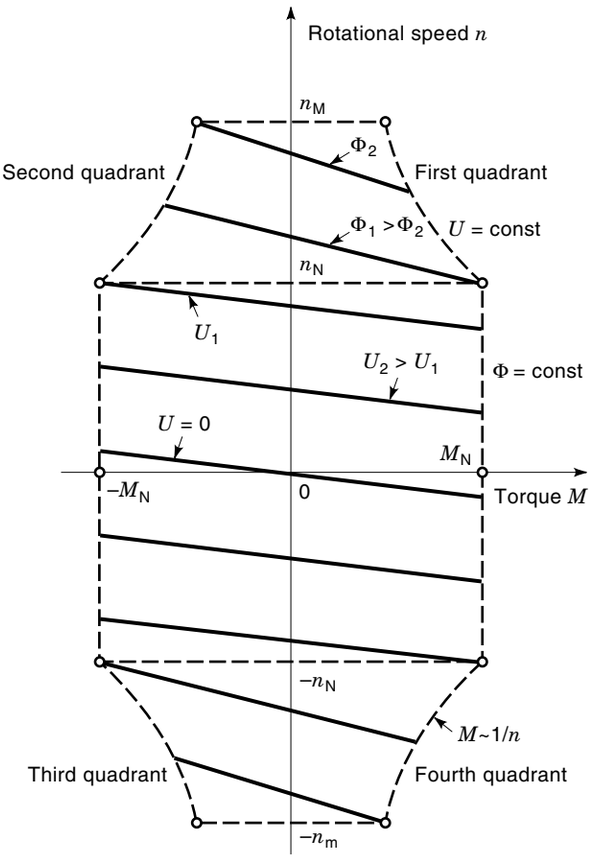

Figure 7. Speed–torque characteristic of separately excited dc machine, fed with variable armature voltage U and fixed flux Φ for $n < n_N$ and with fixed armature voltage U and weakened flux Φ for $n_N < n < n_m$.

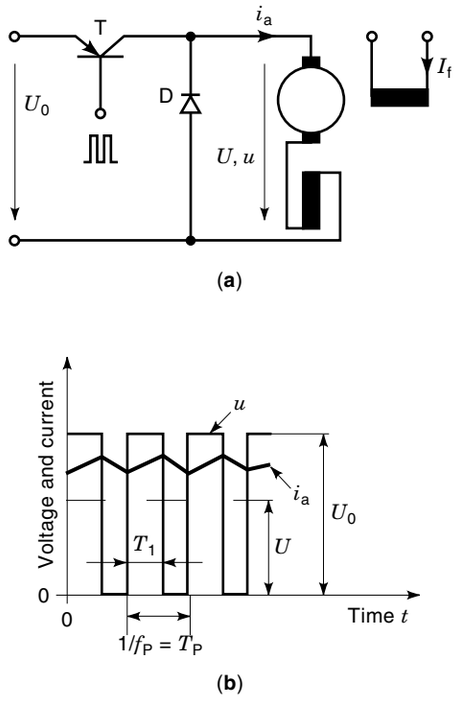

Figure 8. Separately excited dc machine with pulse-width-modulated chopper supply. (a) Chopper circuit for first-quadrant operation. (b) By increasing the duty cycle T_1/T_P the average voltage U is increased.

armature current. Then the firing angles of both converters must be correlated due to Eq. (13) according to

$$\alpha_2 = 180^\circ - \alpha_1 \tag{18}$$

2. Only one converter is active, supplying U, whereas the other one is blocked.

Solution 1 has the advantage of very quick changes of direction in current flow and torque. Note that only the average values of the rectified voltage of both converters are equal, whereas the time functions $u_1(t)$ and $u_2(t)$ are different. Their difference $u_1(t) - u_2(t)$ drives an additional circular current flow through both converter bridges, causing additional losses and temperature rise in the power electronic devices. So, for big drives, solution 2 is preferred at the expense of reduced dynamic performance, when change of torque direction is required (5 ms to 10 ms elapsing time for the changeover between the two converters).

Smaller dc machines (for example, permanent magnet excited machines) are often fed by transistor choppers, being operated with a fixed switching frequency $f_P = 1/T_P$. Larger machines in dc railway drives often use gate turn-off thyristor (GTO) choppers. With GTO choppers for larger currents only low switching frequencies are possible, typically 200 Hz to 500 Hz, whereas with transistors (used for smaller currents) higher switching frequencies of 1 kHz to 3 kHz are typically realized. These choppers operate from a dc link, which is fed, for example, by a six-pulse rectifier from the grid and stabilized by a big capacitance, acting as energy storage and smoothing the 300 Hz (360 Hz) voltage ripple. Figure 8(a) shows a simple chopper for one direction of current flow (first quadrant operation). By varying the duty cycle T_1/T_P (9) from zero to unity [Fig. 8(b)], the average output voltage is varied between 0 and U_0 (pulse-width modulation technique):

$$U = \frac{T_1}{T_P} U_0 \tag{19}$$

Thus again a variable-speed drive is realized. The high switching frequency and the inductance of the armature lead to a rather smooth dc current with only a small superimposed current ripple with the basic frequency f_P. The ripple reaches its maximum peak-to-peak value at $T_1/T_P = 0.5$. During the time T_1 the transistor (T) is active, whereas during $T_2 = T_P - T_1$ the free-wheeling diode (D) is active. Four-quadrant operation is possible if a B2 bridge, consisting of four transistors and four free-wheeling diodes, is provided.

CONTROL

A speed-controlled dc drive needs a tachometer or speed sensor coupled to the rotating machine to measure the actual speed value (7). The speed controller determines the difference $n^* - n$ between the speed setpoint value n^* and actual value n, producing as an output signal the setpoint value I_a^* for the armature current controller (Fig. 9). The actual current value is usually measured on the ac side by current transformers and a rectifier bridge to get a voltage signal, which corresponds to the dc current value I_a. In the case of a controlled silicon rectifier supply, the current controller determines the necessary firing angle α, depending on the difference $I_a^* - I_a$. In case of a pulse-width modulated dc chopper supply, the current controller determines the duty cycle of the chopper. Thus, the dc machine is supplied with the necessary armature voltage U, Eq. (13), to adjust the desired speed n^* and the armature current I_a^*. The structure of control is the so-called cascaded controller with the speed controller acting on the current controller. The time constant for the change of armature current is determined mainly by the time constant of the armature winding T_a, Eq. (23). Change of speed is influenced mainly by the mechanical time constant T_m, which increases with increasing moment of inertia J of the rotating

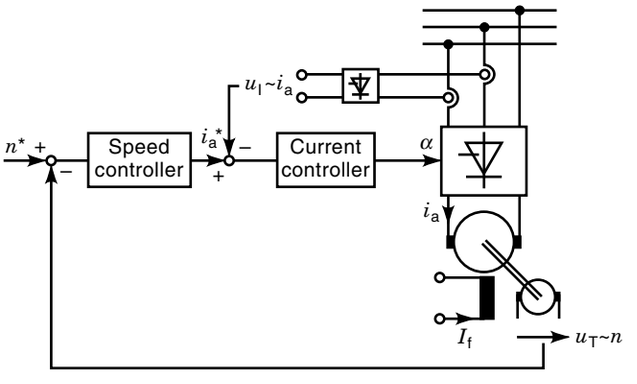

Figure 9. Speed and current control loop of a converter-fed, separately excited dc machine with tacho generator T (output voltage u_T) for speed sensing and current transformers with rectifier bridge (output voltage u_l) for dc sensing.

masses and decreases with increasing magnetic flux, Eq. (24). As T_a is much shorter than T_m, the settling time of the current controller is much shorter than that of the speed controller. This is necessary, because for proper function of a cascaded controller the settling time of the underlying controller must be considerably shorter than that of the master controller. From Eqs. (5), (7), and (8) one derives the dynamic equations (20) and (21), considering now also time-varying armature voltage u, current i_a, speed n, and load torque m_l:

$$L_a \frac{di_a}{dt} + R_a i_a + kn\Phi = u \tag{20}$$

$$J2\pi \frac{dn}{dt} = \frac{k}{2\pi} i_a \Phi - m_l \tag{21}$$

$$\frac{d^2 i_a}{dt^2} + \frac{1}{T_a}\frac{di_a}{dt} + \frac{1}{T_a T_m} i_a = \frac{k\Phi}{2\pi}\frac{1}{JL_a} m_l + \frac{1}{L_a}\frac{du}{dt} \tag{22}$$

$$T_a = \frac{L_a}{R_a} \tag{23}$$

$$T_m = \frac{JR_a}{\left(\frac{k\Phi}{2\pi}\right)^2} \tag{24}$$

Combining Eqs. (20) and (21) yields Eq. (22), where $u(t)$ is the manipulated variable of the control circuit, whereas $m_l(t)$ denotes the disturbance. The response characteristic of a dc machine with constant main flux, for example, to an increase of load torque M_l may be described by the time constants T_a and T_m. The response of the armature current to a step of armature voltage ΔU at $t = 0$ is derived from Eq. (20). With $i_a(t) = I$ for $t < 0$ and $i_a(t) = I + i$ for $t > 0$ one gets

$$i(t) = \frac{\Delta U}{R_a}\left[1 - \exp\left(-\frac{t}{T_a}\right)\right] \tag{25}$$

In the same way the increase of speed due to a sudden reduction in load torque (at $t = 0$ load step-ΔM_l) is determined by Eq. (21), and—considering $T_a \ll T_m$—one gets for the change of speed Δn, if n was the speed for $t < 0$ and $n + \Delta n$ is the speed for $t > 0$,

$$\Delta n(t) = \frac{\Delta M_l T_m}{2\pi J}[1 - \exp(-t/T_m)] \tag{26}$$

With Eqs. (20) to (24) controller design is accomplished (for example, PID controller for the speed loop and PI controller for the current loop).

Control used to be realized by analog circuits, but is now done digitally to benefit from improved possibilities in incorporating mathematical sophisticated models for so-called technology controllers, for example, for cranes, winders, and mills. The influence of drifts and offsets in digital controllers is much smaller than that in analog controllers, and there is good reproducibility. Computing time and analog-to-digital conversion time are steadily decreasing with the progress of microcomputers and electronic devices so that dynamic performance of digital control is now sufficient for many technical applications. Moreover, with six-pulse converter-fed dc drives the cycle time of the digital control is not the limit for dynamical performance of the control. The limit is given by the time $1/6f$ (3.3 ms at 50 Hz or 2.8 ms at 60 Hz), which is the period of the current ripple. This time is needed to calculate the average current value in order to eliminate the influence of the superimposed current ripple on the control performance. Therefore the minimum current rise time of the controller output is $1/6f$. With chopper control this limit is not given. Drives with pulse-width modulation of sufficient high switching frequency therefore have a higher dynamic performance. Thus servo drives for tooling machinery are preferably permanent magnet dc machines with chopper control. These drives are now replaced by permanent magnet synchronous machines with chopper control, which is triggered by a rotor position sensor. With these machines the pulse-width-modulated inverter along with the rotor position sensor may be regarded as the replacement of the mechanical commutator, and the three-phase stator armature winding of these synchronous machines corresponds to the rotor armature of the dc machines. The advantage of the synchronous servo drives is the lower rotor moment of inertia due to the lack of the mechanical commutator, yielding better dynamical performance, as T_m is lower, and the low maintenance due to the lack of brushes. Therefore these drives are called *brushless* dc drives (7).

The cascaded speed control is usually extended by an emf controller (field-weakening controller). If the measured speed n surpasses rated speed n_N, this controller—by using the no-load characteristic (Fig. 3) as a numerical table—generates a new setpoint value I_f, which is lower than the rated value I_{fN}, for the underlying I_f-current controller. This controller generates the necessary firing angle α_f for the controlled rectifier bridge of the field-current circuit [Fig. 6(a)], thus applying a voltage U_f to the field winding, which drives the wanted field current I_f. The electromagnetic time constant T_f of the field circuit

$$T_f = \frac{L_f}{R_f} \tag{27}$$

defined by the inductance L_f and the resistance R_f of the field winding, is much larger than the armature time constant T_a due to the big main flux linkage, as the number of turns per field coil N_f of separately excited dc machines is much larger than that of the armature winding. Therefore speed control is done preferably by the armature circuit control due to its better dynamical performance than with the rather slow field circuit, which is only used to extend the speed range when the armature voltage limit is reached.

For mathematical modeling of the drive to get an accurate parameter design of the controller, not only electromagnetic but also mechanical properties of the motor–drive set have to be considered in detail. So, if necessary, elastic coupling (10), torsional vibrations of long shaft connections, which might be excited by the ac ripple of the torque due to the motor current ripple, and other influences have to be taken into account.

ARMATURE COILS

The single armature coil of Fig. 1 is of the lap winding type. In Fig. 10(a) an example with $K/(2p) = 14$ commutator segments between two brushes of opposite electric potential is depicted, resulting in 14 series-connected lap-type coils between plus and minus brush. In reality the number of series-

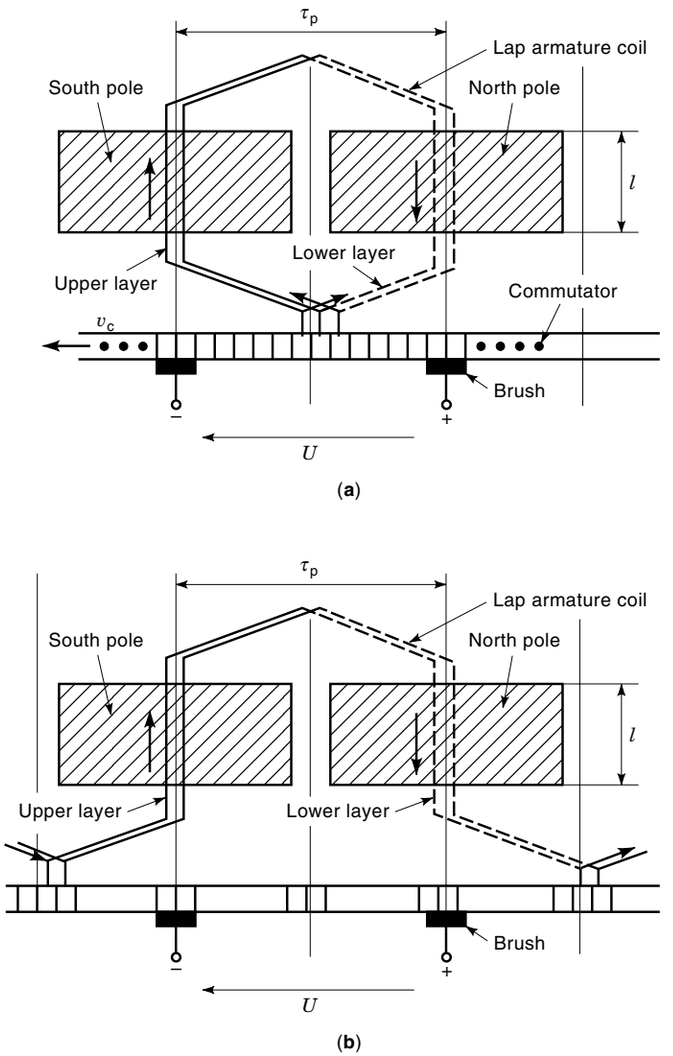

Figure 10. Schematic sketch of armature winding with connection to the commutator segments (stator pole shoes depicted as shaded areas). (a) Simplex lap winding. (b) Simplex wave winding (four-pole machine assumed).

connected coils between the brushes is 30 to 40 for a medium-power dc machine to achieve a low-voltage ripple of 1% to 2% of rated voltage [Fig. 1(d)] (11,12). The commutator pitch of the coil Y_c, expressed in number of segment pitches, is 1, as adjacent segments are connected to one coil. As the brush coverage ratio of commutator segments, defined by the ratio of brush width versus segment width, is usually designed between 2 and 5, two to five of the $K/(2p)$ series-connected coils are always short-circuited by the brushes. During this short-circuit time T_s the armature coil current has to reverse its direction of current flow. The coil voltage that is short-circuited is low, as during short circuit the coil passes the neutral zone, where the inducing air gap field is nearly zero [Fig. 1(c)]. A four-pole dc machine has four adjacent brushes distanced along the commutator circumference by one pole pitch, two of positive and two of negative electric polarity. Brushes of the same polarity are connected in parallel. Therefore the armature winding consists of four parallel electric circuits, yielding in general the following law for simplex lap armature windings (a is the number of parallel paths per half armature):

$$2a = 2p \tag{28}$$

Magnetic asymmetries of different main poles cause slight differences between the induced voltages of different parallel paths. These differences can be equalized by connecting points of the same electric potential of different parallel paths with so-called equalizers, usually one connection per rotor slot. As one parallel path of simplex windings is usually designed for currents up to 500 A with limits due to the available slot cross section and the current density in the slot copper bars, all larger machines are designed with lap windings (13). Very big machines used to have duplex lap windings, consisting of two independent lap windings, each having a commutator pitch $Y_Q = 2$. Parallel connection of both lap windings is accomplished by the brushes and additional equalizers to compensate voltage differences due to asymmetries. Thus the number of parallel paths is twice that of simplex windings.

For smaller output power the simplex wave armature winding is preferred, which has only $2a = 2$ parallel paths, independent of the number of pole pairs p of the machine [Fig. 10(b)]. This is accomplished by a waveform shape of the coils, which connect commutator segments, that are distanced by nearly two pole pitches (11,12). The coil span is given by

$$Y_Q = \frac{K-1}{2p} \tag{29}$$

With only two parallel paths it is sufficient to use only one brush pair (one plus and one minus brush). In practice in most cases p brush pairs are used, just as in the case with lap armature windings. The main reason is that the steady-state brush current density is limited to typically 10×10^4 A/m^2 to 12×10^4 A/m^2 (14). Thus the brush coverage ratio of commutator segments with only two big brushes would be too large. Two positive parallel-connected brushes, distanced with two pole pitches $2\tau_p$, are short-circuiting only one coil if the brush coverage ratio is 1, or two coils if the ratio is two and so on, so it is possible to arrange the brushes in the same way as with lap windings. With smaller dc machines wave armature windings are well suited, because with only two parallel paths the number of turns in series of the armature is large enough to reach the rated voltage of typically 400 V to 600 V even with a small air-gap flux per pole Φ.

Apart from very small dc machines with rated steady-state power below typically 1 kW, usually an auxiliary winding is needed, the so-called *compole* winding. It is necessary to ensure "dark" commutation of the armature coil current. This means that reversing the polarity of coil current when the coil is short-circuited by the brushes [Fig. 11(a)], is possible without heavy sparking at the trailing edge of the brush, when the brush–commutator segment mechanical contact opens. The change of the ac coil current i_c during the short-circuit time T_s, given by the brush width b and the commutator circumferential speed v_C,

$$T_s = \frac{b}{v_C} \tag{30}$$

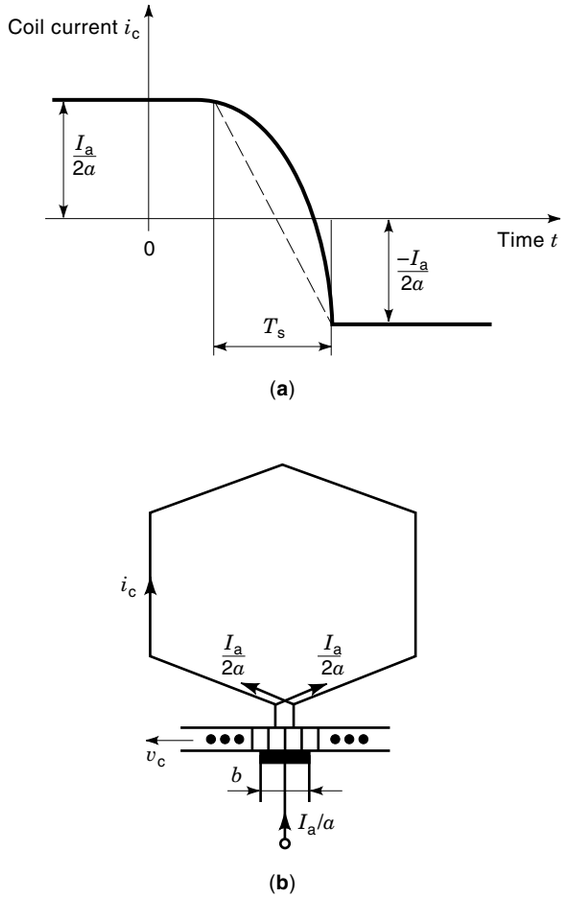

Figure 11. Commutation of armature coil current i_c. (a) The coil current has to reverse its polarity, while the coil is short-circuited by the brush. (b) The commutating lap coil is short-circuited by the brush.

from $+I_a/(2a)$ to $-I_a/(2a)$ and vice versa, causes a reactance voltage u_r due to the inevitable coil stray inductance L_c [Fig. 11(b)]:

$$u_r = L_c \frac{di_c}{dt} \cong L_c \frac{I_a}{aT_s} \propto nI_a \tag{31}$$

This voltage causes ignition of sparks at the brush's trailing edge, causing wear of the brush and the commutator, thus reducing the brush life drastically. The ideas of the compole winding is to excite an additional air-gap field B_C in the neutral zone between two adjacent main poles, which opposes the armature reaction field. Thus u_r can be compensated by an additional voltage u_C, which is induced in the commutating coil due to the movement of the armature with speed v in the compole field B_C:

$$u_C = 2N_c B_C l v \tag{32}$$

The compensation must be accomplished at any speed n and load I_a to ensure dark commutation for any arbitrary load:

$$u_C = u_r \propto nI_a \tag{33}$$

This goal is reached by feeding the coils of the compoles (Fig. 12) with the armature current I_a. As the armature reaction mmf $N_A I_a$ (N_A is the armature windings per pole) has to be overcome by the compole mmf $N_C I_a$ (N_C is the number of turns per compole) to generate a resulting air-gap compole flux density B_C, the ratio N_C/N_A is usually chosen as 1.12 to 1.25. Adjustment of B_C is accomplished by the proper choice of N_C and by adjusting the compole air gap δ_C with additional iron sheets during the final test in the manufacturer's shop (15). It is necessary, that the magnetic path for B_C is unsaturated to obtain the relationship $I_a \propto B_C$; this should be ensured up to twice the rated armature current.

$$B_C \propto \frac{(N_C - N_A)I_a}{\delta_C} \tag{34}$$

Big machines with an output power higher than typically 200 kW to 300 kW are equipped in addition with a series-compensating winding, which is fixed in slots in the pole shoes of the stator poles (Fig. 12). This winding is also loaded by the armature current, thus exciting an air-gap field, which opposes the armature reaction field. By adjusting the number of turns of the coils of the compensating winding in relation to those of the armature coils and by choosing a slot pitch that is similar to the rotor slot pitch, but not identical to avoid cogging, it is possible to extinguish the armature reaction field with its negative influence on the machine (16). The auxiliary windings do not play an active part in electrical energy conversion, but cause additional ohmic losses. Thus, along with the rotor iron losses, the electrical brush losses, the brush friction losses, the eddy current losses in the armature coils due to the ac coil current, and the converter-induced current ripple (17), these losses yield a slightly lower machine efficiency when compared with ac induction and synchronous machines (18).

TEMPERATURE CONTROL

There exist many different cooling systems for electrical machines (19); dc machines are manufactured often with open-circuit cooling. The cooling air flow enters the dc machine usually through openings in the end shield at the nondrive end side, where the commutator is situated, and passes through axial and radial ventilation ducts of the rotor and through the axial gaps in the stator between the main poles, leaving the machine through openings in the drive-end end shield (20). For variable-speed drives an external fan to generate a constant, speed-independent air flow is necessary. A fan mounted on the rotor shaft of the machine itself would deliver an insufficient air flow at low motor rotational speed. The different windings of the dc machine (armature, field, compole, compensation) and the surface of the commutator with the brushes are cooled intensively with the cool air entering on the commutator side, passing closely to the surface of the windings. This method ensures a high utilization of the machine, resulting in a compact build, but causes a rather large temperature gradient of typically 20 K to 40 K between the cool-air inlet and the hot-air outlet, where the heated air flow leaves the machine. The hot spots in the coils are therefore located on the hot outlet side, so the temperature sensors are fixed to the windings also on the hot side. In separately

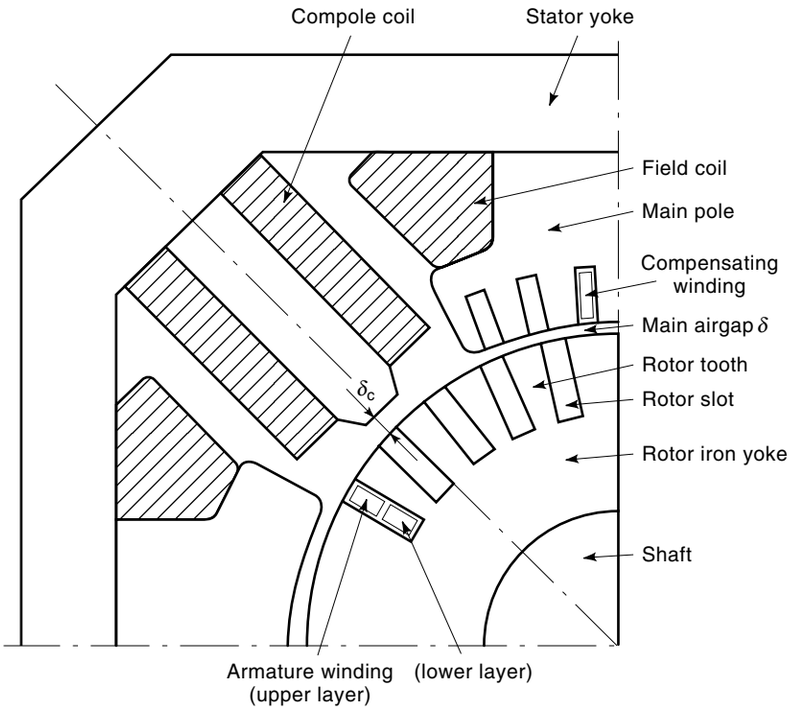

Figure 12. Cross section of a four-pole dc machine with rotor armature winding, stator field, compole, and compensating winding (main air gap δ and compole air gap δ_C enlarged for clarity).

excited dc machines usually one sensor is necessary for the compole winding and one for the field winding. The rotating armature winding would need additional sliding contacts or a wireless signal transmission if a temperature sensor were placed into this winding. So the compole temperature sensor is also used to protect the armature winding, as both windings are loaded with the same armature current, which causes the copper losses P_d as dissipated heat along with the temperature rise $\Delta\vartheta$:

$$\Delta\vartheta \propto P_d = RI_a^2 \tag{35}$$

One has to consider that the heating of the armature winding is caused not only by load losses, Eq. (35), but also by main flux-dependent losses in the active iron core. By careful design of armature and compole winding one tries to obtain nearly the same steady-state temperature rise in both windings. So it is possible to protect the armature winding with the compole sensor and yet utilize both windings to their temperature limit. This limit is given by the thermal limit of the utilized insulation material of the electrical winding (21). For example, insulation class F material sustains a steady-state temperature rise of 105 K in addition to 40°C ambient temperature plus 15 K additional temperature rise in hot spots, resulting in a maximum temperature of 160°C, for at least 20,000 h, de facto for a much longer period of time. The corresponding temperature control is designed for insulation class F usually with an operating temperature of 105°C + 40°C = 145°C. Tripping miniaturized bimetal temperature relays and semiconductor components such as negative temperature coefficient (NTC) and positive temperature coefficient (PTC) elements are used as protective sensors. For continuous temperature measurement thermocouples or platinum resistance elements are utilized. Good thermal contact between sensor and copper wire is necessary to ensure a low thermal time constant of the sensor measuring system (several seconds) and a similar temperature rise of winding and sensor. So, the sensors are usually put between the wires of the windings. After this, the winding is impregnated with epoxy resin to get good electric insulation and protection against humidity and carbon dust. In addition to temperature sensors, often the air flow itself is controlled directly by an air-pressure sensor at the air-flow inlet.

TIME-VARYING LOADS

As already stated, the resulting inductivity of the armature L_a is rather low, yielding a low electrical time constant T_a, giving the dc drive good dynamical performance, which is necessary especially under time-varying load conditions. The reason for the low inductance is that the compole winding (or compole and compensating winding) with inductance $L_C \propto N_C^2$ on one hand and the armature winding with inductance $L_A \propto N_A^2$ on the other hand excite air-gap fields, which oppose each other. Thus the inductive coupling of this pair of windings, given by the mutual inductance $M_{AC} \propto N_A N_C$, yields a low resulting inductance L_a for the whole armature circuit (Fig. 13).

$$L_A = L_{A\sigma} + L_{Am} \tag{36}$$

$$L_C = L_{C\sigma} + L_{Cm} \tag{37}$$

$$L_a = L_A - M_{AC} + L_C - M_{AC} \tag{38}$$

$$L_a = L_{A\sigma} + L_{C\sigma} + \left(1 - \frac{N_C}{N_A}\right)^2 L_{Am} \tag{39}$$

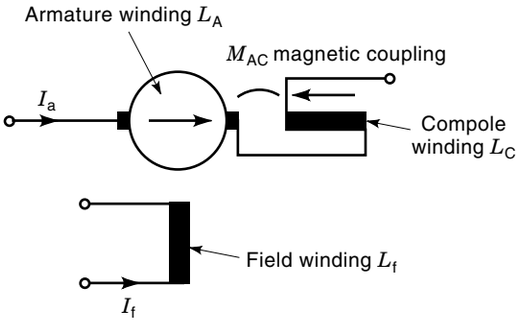

Figure 13. The compole (and compensating) winding excites a magnetic field that opposes the armature reaction field, yielding a low resulting inductance. The field winding is not magnetically coupled with these windings (besides saturation cross-coupling).

As N_C/N_A is typically 1.12 to 1.25, L_a represents mainly the stray inductance of the rotating armature and of the compole winding $L_{A\sigma}$ and $L_{C\sigma}$, thus explaining its low value.

Change of Load Current

Modern dc machines are designed usually to sustain sudden load peaks of twice the rated armature current for several seconds (22). One limit is given by avoiding saturation of the compole magnetic circuit when the linearity between armature current and compole field, Eq. (34), would be lost with large armature currents, yielding too weak a compole field B_C. A second limit is the brush current density, for brushes can sustain current densities of about 20×10^4 A/m^2 only for several seconds without being overheated. The rate of change of the armature current can be very large if the compole magnetic paths consist completely of laminated iron parts ($di_a/dt \leq 600 I_N$ per second, typically), as eddy currents in the iron core are suppressed. Older machines with massive iron yokes suffer from a delay of the compole flux change due to the intrinsic magnetic field of the eddy currents in the massive iron parts, causing too weak a compole field under transient load conditions (16). Thus with these machines the rate of current change is limited to $20 I_N$ per second.

Change of Speed

At standstill the load current has to be reduced to stay well below the 6×10^4 A/m^2 brush current density to avoid burning-in on the commutator surface.

Load Cycles

Thermal time constants of the machine depend on the machine size and on the cooling condition. Small machine and machines with a forced open-circuit cooling usually have lower time constants than large machines or machines with surface cooling. The stator windings may be described by one thermal time constant for each winding system, whereas for the armature winding a shorter and a longer time constant have to be taken into account, as two different loss sources have to be considered, namely the current-dependent copper and additional losses and the flux-dependent iron losses. Usually one tries to evaluate one single equivalent thermal time constant. For example, a four-pole 100 kW dc machine with forced open-circuit cooling will have an armature circuit equivalent thermal time constant of typically 15 min to 30 min. The temperature rise in dc machines with intermittent load with a load-cycle duration longer than only a few seconds is determined by the thermal time constants of the machine. Such a situation is typical for elevators and cranes (for example, 10 min cycle time, 6 min load, and 4 min no-load period). Thus with intermittent periodic duty higher motor currents are permissible than under steady-state conditions, as the temperature decreases during the no-load period. As an equivalent measure for the temperature of the windings the temperature rise in the middle of the load period is taken (18).

LIMITS OF DC MACHINES

Torque Limit

The delivered electromagnetic torque M for a given current load A and air-gap induction B is determined by the main geometric data (11,16) d [diameter of the armature at the surface, Fig. 1(b)] and l [iron stack length of the core, Fig. 1(b)], Eq. (40), which is derived from Eqs. (6) and (7). Therefore a machine designed for big torque usually has a large diameter.

$$M = \frac{\pi}{2} \alpha_e d^2 l A B \tag{40}$$

Modern dc machines are designed for high utilization to keep the ratio of investment costs to installed power as low as possible. A high output torque per motor volume can be achieved by increased current load and by increased air-gap induction. The latter is limited due to the saturation of the rotor teeth to about 1 T. High current load with limits of typically 50 kA/m (11) is accomplished by optimized cooling and by designing the machines for a higher steady-state temperature rise through use of improved materials.

Speed Limit

A high output power can be obtained by an extended speed range according to Eq. (17). Whereas A and B set nearly the same limits also on ac machines, dc machines are more sensitive to high speed than ac machines. Speed limits are caused by the electrical commutation of the armature current and by the mechanical speed limit of the commutator.

1. The critical mechanical speed due to the centrifugal forces of the commutator copper segments is an upper speed limit for dc machines (23).
2. At high speed the brushes no longer slide smoothly on the commutator surface. Brush chatter, which is a high-frequency bending vibration of the brush, and brush jumping may occur with a rapid increase of mechanically induced brush wear (14).
3. The reactance voltage u_r rises linearly with speed, Eq. (31). So, sparking will occur preferentially at high speed, causing increased electrically induced brush wear. Therefore above a critical speed n_f, corresponding to a maximum value of u_{rm} of about 8 V to 10 V, the armature current has to be reduced, Eq. (41). Therefore modern variable-speed dc drives have a steady-state

load characteristic as depicted in Fig. 14. For example, the maximum speed n_m of a 100 kW dc machine (shaft height 160 mm, n_N = 2000/min) lies typically between 4500/min and 6000/min, depending on the mechanical rotor design, corresponding with an overspeed test of 120% of n_m for 2 min.

$$I_a \propto \frac{u_{rm}}{n} \tag{41}$$

Highly utilized dc machines with considerable high magnetic flux densities in the stator yoke (Fig. 12) suffer from saturation of the stator yoke due to the main flux. As both main and compole flux pass through the same parts of the stator yoke, the compole flux is also saturated to a certain extent. Beyond rated speed, when the main flux is weakened, the yoke returns to the unsaturated state, resulting in an increase of the compole air gap flux density B_C. The compole voltage u_C then overcompensates the reactance voltage u_r at high speed, causing sparking of the brushes.

All these negative influences on commutation can be encountered partially by designing improved armature windings, which are more insensitive to commutation disturbances. Examples of measures to improve commutation are the design of a low coil inductance L_c to get a low reactance voltage. Reduced slot height to get low slot leakage inductance and the use of split-throw windings (24,25) (necessary for rated power above typically 200 kW) yield low coil inductances. The last coil per slot has the highest coil inductance L_c due to lack of magnetic coupling with other short-circuited commutating coils of the same slot. Therefore its commutating condition is worse than that of the other coils. Equalizers connect the last coil per slot with coils of the same electric potential. Thus those coils, which are distanced by two pole pitches, produce unavoidable magnetic asymmetries of the machine, which cause different sparking of certain brushes. For machines with both rotation directions, the first and the last coil per slot must be connected to equalizers, of course, yielding $2Q/p$ equalizers ($p > 1$). Moreover, by obtaining deeper insight into the physical nature of the brush–commutator contact, further improvements are possible (26).

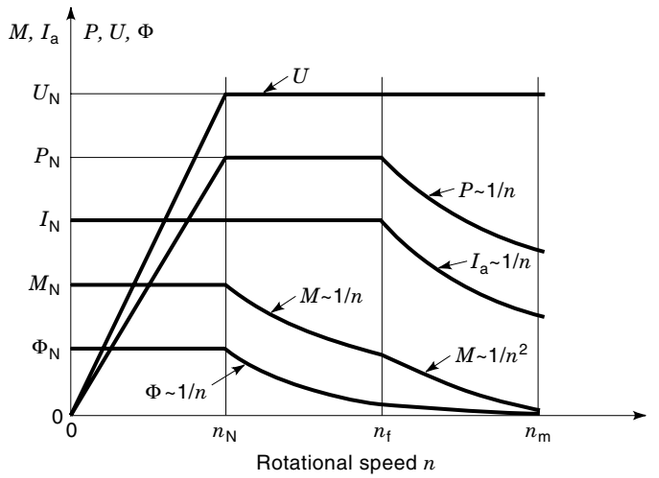

Figure 14. The dc motor as a variable-speed drive, being fed by variable armature voltage U and variable main flux Φ. At high speed $n > n_f$ the output power P has to be reduced to limit the reactance voltage of commutation.

Voltage Limit

The mechanical commutator puts also a limit to the armature voltage. The average bar-to-bar voltage between to commutator segments u_s must stay below 18 V (uncompensated machines) and 20 V (compensated machines) to avoid flashover already at no-load conditions. With a load there is a distortion of the air-gap flux density distribution due to armature reaction with uncompensated machines, yielding a maximum bar-to-bar voltage u_m, which is considerably higher than the average value especially at considerable flux weakening, thus at high speed. This maximum value should stay below 35 V. With a minimum commutator pitch of about 3.5 mm, needed for connecting the armature coil ends to the segment, and a minimum mica insulation thickness of about 0.8 mm to ensure the just noted voltage limits, maximum armature voltages of typically 1000 V are reached. Larger voltages would yield large commutator diameters due to the large number of segments between two brushes, which again would be critical to centrifugal forces.

These limits are the reason why there is now a strong trend to change from dc drive technology, especially with high-speed application, to ac drives with the robust induction motor and the "brushless" dc motor. Nevertheless, for medium speeds up to typically 4000/min in the power range of 100 kW to 1000 kW dc drives are still a solution of high technical maturity with a reasonable ratio of investment cost to output power and an excellent dynamical performance for many technical applications, and will remain of economical importance for years to come (27).

BIBLIOGRAPHY

1. J. Hindmarsh, *Electrical Machines and their Applications,* 4th ed., Oxford: Pergamon, 1991.
2. J. Hindmarsh, *Electrical Machines and Drives—Worked Examples,* 2nd ed., Oxford: Pergamon, 1991.
3. N. Carver, Aspects of carbon brush performance, *Elevator World,* (Feb.): 60–69, 1990.
4. F. J. Bartos, DC drives still have miles to go before they sleep, *Control Eng.,* (Aug.): 48–50, 1991.
5. R. Robbins, DC will continue as viable drives technology option, *Drives Controls,* (Mar.): 60–61, 1997.
6. A. Kusko and S. M. Peeran, Application of 12-pulse converters to reduce electrical interference and audible noise from DC motor drives, *IEEE Trans. Ind. Appl.,* **29**: 153–160, 1993.
7. W. Leonhard, *Control of Electrical Drives,* 2nd ed., Berlin: Springer, 1996.
8. B. K. Bose (ed.), *Modern Power Electronics—Evolution, Technology, and Application.* New York: IEEE Press, 1992.
9. J. M. D. Murphy and F. G. Turnbull, *Power Electronic Control of AC Motors,* Oxford: Pergamon, 1988.
10. W. Hulsbosch et al., Influence of the Elastic Coupling on the Control of Converter Fed DC Motor Drives, *Proc. 3rd Eur. Conf. Power Electron. Appl. (EPE),* Aachen, Germany, 1989, pp. 849–854.
11. K. Vogt, *Berechnung rotierender elektrischer Maschinen,* Weinheim, Germany: VCH, 1996.
12. J. Schneider, Elektrische Entwurfsberechnung, in W. Böning (ed.), *Hütte-Elektrische Energietechnik,* Band 1: *Maschinen,* 29. ed., Berlin: Springer, 1978.

13. A. Binder, Comparison of the electromagnetical performance of simplex wave and lap windings, *IEEE Trans. Energy Convers.* **8**: 698–703, 1993.
14. E. I. Shobert, *Carbon Brushes,* New York: Chemical Publishing, 1965.
15. G. M. J. Parsley, A. S. Meyer, and C. F. Landy, Factors affecting the prediction of commutating limits for a DC machine under varying speed and load conditions, *Trans. South African Inst. Electric. Eng.,* (Sept.): 171–176, 1992.
16. W. Dull, Gleichstrommaschinen, in W. Böning (ed.), *Hütte-Elektrische Energietechnik,* Band 1: *Maschinen,* 29. ed., Berlin: Springer, 1978.
17. A. Binder, Additional losses in converter fed uncompensated dc machines-their calculation and measurement. *Electric. Eng. (Archiv für Elektrotechnik)* **74**: 357–369, 1991.
18. Rotating electrical machinery, Part 2: Methods for determining losses and efficiency of rotating electrical machinery from tests (excluding machines for traction vehicles), *IEC Publication IEC 34-2,* Geneva: IEC Central Office, 1972.
19. W. Liebe, Entwärmung elektrischer Maschinen, in W. Böning (ed.), *Hütte-Elektrische Energietechnik,* Band 1: *Maschinen,* 29. ed., Berlin: Springer, 1978.
20. R. Schamberger and E. Thum, DC Machines of Rectangular Construction for Torques from 300 to 3000 Nm, *Siemens Power Eng.,* **3**: 17–21, 1981.
21. Rotating electrical machinery, Part 1: Rating and performance, *IEC Publication IEC 34-1,* Geneva: IEC Central Office, 1994.
22. J. D. White, M. Zeller, and W. Goss, *DC Motors for Variable Speed Drives, Catalog DA12,* Erlangen, Germany: Siemens AG, 1992.
23. I. Huszár, Bemerkungen zur Wahl des Gewölbedrucks von Kommutatoren, *Elektrische Bahnen* **36**: 291–296, 1965.
24. W. J. Pratt, The influence of design parameters on the sparkless zones of dc machines, *GEC J. Sci. Technol.,* **45**: 51–55, 1978.
25. A. Binder, Measures to raise brush life of modern dc machines, *Eur. Trans. Electric. Power Eng.,* **3**: 193–200, 1993.
26. G. N. Friedman and T. I. Fomicheva, Effect of commutator conductor materials on commutation of electric machines, *Elektrotekhnika* **60**: 32–36, 1989 (reprinted by Allerton Press, 1989).
27. E. Auernhammer et al., Kompakte Gleichstromantriebe durch Leistungssteigerung, *Elektrotechnische Z.,* **113**: 1342–1349, 1992.

ANDREAS J. F. BINDER
Darmstadt University of Technology

DC OPERATING POINTS. See HIGH DEFINITION TELEVISION; HOMOTOPY METHODS FOR COMPUTING DC OPERATING POINTS.

DCT. See HADAMARD TRANSFORMS.